ORIGINAL RESEARCH

An Alternative Spirometric Measurement

Area under the Expiratory Flow–Volume Curve

Octavian C. Ioachimescu[1] and James K. Stoller[2]

[1]Division of Pulmonary, Allergy, Critical Care and Sleep Medicine, School of Medicine, Emory University, Atlanta VA Sleep Medicine Center, Atlanta, Georgia; and [2]Respiratory and Education Institutes, Cleveland Clinic, Cleveland, Ohio

ORCID ID: 0000-0001-9047-6894 (O.C.I.).

Abstract

Rationale: Interpretation of spirometry is influenced by inherent limitations and by the normal or predicted reference values used. For example, traditional spirometric parameters such as "distal" airflows do not provide sufficient differentiating capacity, especially for mixed patterns or small airway disease.

Objectives: We assessed the utility of an alternative spirometric parameter (area under the expiratory flow–volume curve [AEX]) in differentiating between normal, obstruction, restriction, and mixed patterns, as well as in severity stratification of traditional functional impairments.

Methods: We analyzed 15,308 spirometry tests in subjects who had same-day lung volume assessments in a pulmonary function laboratory. Using Global Lung Initiative predicted values and standard criteria for pulmonary function impairment, we assessed the diagnostic performance of AEX in best-split partition and artificial neural network models.

Results: The average square root AEX values were 3.32, 1.81, 2.30, and 1.64 $L \cdot s^{-0.5}$ in normal, obstruction, restriction, and mixed patterns, respectively. As such, in combination with traditional spirometric measurements, the square root of AEX differentiated well between normal, obstruction, restriction, and mixed defects. Using forced expiratory volume in 1 second (FEV_1), forced vital capacity (FVC), and FEV_1/FVC *z*-scores plus the square root of AEX in a machine learning algorithm, diagnostic categorization of ventilatory impairments was accomplished with very low rates of misclassification (<9%). Especially for mixed ventilatory patterns, the neural network model performed best in improving the rates of diagnostic misclassification.

Conclusions: Using a novel approach to lung function assessment in combination with traditional spirometric measurements, AEX differentiates well between normal, obstruction, restriction and mixed impairments, potentially obviating the need for more complex lung volume-based determinations.

Keywords: spirometry; area under the flow–volume curve; neural networks; machine learning; artificial intelligence

(Received in original form August 15, 2019; accepted in final form January 3, 2020)

Author Contributions: O.C.I.: Conception of the work, data collection and analysis, and manuscript writing. J.K.S.: Conception of the work and manuscript writing.

Correspondence and requests for reprints should be addressed to Octavian C. Ioachimescu, M.D., Ph.D., Atlanta VA Sleep Medicine Center, 250 North Arcadia Avenue, Atlanta, GA 30030. E-mail: oioac@yahoo.com.

Ann Am Thorac Soc Vol 17, No 5, pp 582–588, May 2020

DOI: 10.1513/AnnalsATS.201908-613OC
Internet address: www.atsjournals.org

Interpretation of pulmonary function tests (PFTs) is essentially based on comparing measured flows or volumes against their predicted values derived from healthy individuals from similar populations (1–3). Generally, forced vital capacity (FVC), forced expiratory volume in 1 second (FEV_1), FEV_1/FVC ratio, and total lung capacity (TLC; obtained by body plethysmography, gas dilution, or other methods) are the key variables used to interpret pulmonary function. Measuring or computing residual volume (RV), functional residual capacity (FRC), and TLC is technically complicated and more challenging. Although this may limit the use of these tests in clinical practice, in particular situations they become essential for characterizing the physiological state or impairment (4).

For each lung function measurement or calculated parameter, values at the fifth percentile from healthy sex- and race-referenced individuals define what is considered the lower limit of normal (LLN) (1, 5). This approach, similar to the one using the *z*-scores or "standardized"

variables (i.e., the number of standard deviations away from the mean), assumes that the parameters are part of a normal distribution, which is, in fact, rarely the case. When the frequency distribution is skewed, a nonparametric technique such as the 95th-percentile method can be used instead (6). Nevertheless, unlike percent predicted values, *z*-scores are free from bias induced by age, height, sex, ethnicity, or race and therefore are particularly useful in defining the LLNs and increasingly recommended in the interpretation of PFTs (2).

Two of the most widely used predictive equations are represented by the Third National Health and Nutrition Examination Survey (7) and by predicted reference values for spirometry derived and published by the Global Lung Initiative (GLI) (2). The latter equations are updated and more comprehensive than previous prediction sets and are recommended for implementation in PFT laboratories worldwide; yet, significant adoption variability persists. In addition, significant variability remains in the way PFTs are interpreted, including the best way to define ventilatory impairments beyond obstruction and (possible) restriction.

To address these shortcomings, to potentially enhance the diagnostic accuracy and value of PFTs, and to determine which patients need additional lung volume determinations, in this study, we evaluated the utility of an alternative spirometric parameter called the "area under the expiratory flow–volume curve" (AEX) (8–11). The AEX is the actual integral function of the variable flow (on the *y*-axis) versus expiratory volume (on the *x*-axis) during a forced exhalation maneuver from TLC to RV and is expressed in $L^2 \cdot s^{-1}$ (Figure 1). In this study, AEX was obtained from the proprietary software algorithm of the spirometry equipment's manufacturer. We have previously shown that, in the absence of AEX, several computations based on instantaneous flows may be very close AEX approximations, which could be useful in interpreting observed functional impairment and could potentially be valuable as surrogate measurements (12).

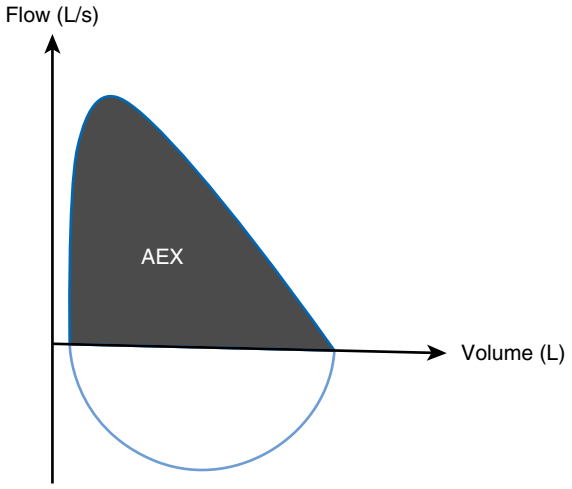

Figure 1. Depiction of the area under the expiratory flow–volume curve (AEX; in $L^2 \cdot s^{-1}$), the integral function of instantaneous flows against expired volume during a forced respiratory maneuver. AEX = area under the expiratory flow–volume curve.

Methods

This data set included a cohort of 15,308 consecutive, best-trial, acceptable, prebronchodilator spirometry tests performed in the Cleveland Clinic PFT Laboratory. The extraction criteria were *1*) prespecified time period of 10 years, *2*) spirometry tests with available AEX values (the largest value was extracted), and *3*) all consecutive tests done in adult subjects who underwent same-day spirometry and lung volume testing by either body plethysmography (13) or a helium dilution technique (14).

Spirometry was performed following the American Thoracic Society (ATS) standards (1, 5, 15). Body plethysmography and helium dilution techniques were used to assess lung volumes per ATS/European Respiratory Society (ERS) standards and criteria (1, 4, 6). Spirometry, body plethysmography, and helium dilution technique determinations were performed using a Jaeger Master Lab Pro system. Reference values from the GLI were used for spirometry interpretation (2). For lung volumes, the reference values used were those of Crapo and colleagues (16). Diagnostic performance of AEX was assessed by the test's receiver operating characteristic curve, accuracy, and reclassification rates. As per the ATS/ERS simplified diagnostic algorithm (6), normal pattern was defined by normal FVC and normal FEV_1/FVC ratio ($FVC > FVC_{LLN}$ and $FEV_1/FVC > FEV_1/FVC_{LLN}$); obstruction was diagnosed either as $FEV_1/FVC < FEV_1/FVC_{LLN}$ and $FVC > FVC_{LLN}$ or as $FEV_1/FVC \geqslant FEV_1/FVC_{LLN}$, $FVC < FVC_{LLN}$, and $TLC > TLC_{LLN}$. A diagnosis of restriction was based on $FEV_1/FVC \geqslant FEV_1/FVC_{LLN}$, $FVC < FVC_{LLN}$, and $TLC < TLC_{LLN}$, whereas a mixed defect was diagnosed if the following conditions were met: $FEV_1/FVC < FEV_1/FVC_{LLN}$, $FVC < FVC_{LLN}$, and $TLC < TLC_{LLN}$. Of note, the interpretation of PFTs was based, in our study and per ATS/ERS recommendations, on both spirometry and lung volumes, the latter being considered the gold standard and necessary differentiator test in a great number of situations.

The AEX (Figure 1) was computed by the available PFT software as the integral function of the exhalation phase of the flow–volume curve. The largest AEX value of all prebronchodilator trials has been selected. For several analyses and models, owing to its nongaussian distribution, the square root of AEX (Sqrt AEX) was used.

We built several models that evaluated the relationships between AEX and inspiratory capacity (IC), FRC, RV, and TLC. We were especially interested in assessing AEX against indices of gas trapping and hyperinflation, such as FRC/TLC or RV/TLC and IC/TLC ("inspiratory fraction"), which can only be derived from lung volume testing. The IC/TLC was shown in prior investigations to be an independent predictor of respiratory and all-cause mortality in subjects with chronic obstructive pulmonary disease. Furthermore, we resorted to several recursive partitioning models with 33% holdback for validation, by which we performed the interactive best-split procedure of the functional diagnostic

Table 1. Demographic characteristics and pulmonary function test measurements ($N = 15{,}308$)

Parameter	Mean ± SD	Median	25th–75th IQR
Age, yr	56 ± 14	57	47 to 67
Height, cm	168 ± 10	168	161 to 175
Weight, kg	81 ± 21	79	66 to 94
Body surface area, m^2	1.9 ± 0.2	1.9	1.7 to 2.0
Body mass index, kg/m^2	28 ± 7	28	24 to 32
FET, s	12.19 ± 3.06	12.86	9.52 to 14.93
PEF, L	5.07 ± 2.49	4.84	3.07 to 6.76
FVC, L	2.94 ± 1.07	2.81	2.14 to 3.59
FVC *z*-score	−1.69 ± 1.61	−1.56	−2.65 to −0.61
FEV_1, L	1.87 ± 0.95	1.77	1.09 to 2.49
FEV_1 *z*-score	−2.50 ± 1.8	−2.37	−3.8 to −1.13
FEV_6, L	2.55 ± 1.02	2.40	1.81 to 3.07
FEV_1/FVC	0.62 ± 0.19	0.62	0.47 to 0.78
FEV_1/FVC *z*-score	−2.31 ± 3.35	−1.59	−4.4 to 0.12
FEV_1/FEV_6	0.65 ± 0.16	0.70	0.51 to 0.79
TLC, L	5.52 ± 1.74	5.30	4.26 to 6.57
RV, L	2.49 ± 1.42	2.07	1.46 to 3.18
RV/TLC	0.43 ± 0.15	0.41	0.32 to 0.54
IC, L	2.13 ± 0.83	2.03	1.52 to 2.63
IC/TLC	0.40 ± 0.12	0.41	0.30 to 0.49

Definition of abbreviations: FET = forced expiratory time; FEV_1 = forced expiratory volume in 1 second; FEV_6 = forced expiratory volume in 6 seconds; FVC = forced vital capacity; IC = inspiratory capacity; IQR = interquartile range; PEF = peak expiratory flow; RV = residual volume; SD = standard deviation; TLC = total lung capacity.

categories as nominal variables. For the recursive partitioning, the following factors were used: FEV_1, FVC, and FEV_1/FVC percent predicted; FEV_1, FVC, and FEV_1/FVC *z*-scores (all determined by race, sex, age, and height); actual FEV_1/FVC; and (Sqrt) AEX. We found that the neural network models using Sqrt AEX, FEV_1, FVC, and FEV_1/FVC *z*-scores performed best (i.e., highest R^2 and area under the receiver operating characteristic curve, dominant pattern probability or density >50%, minimized misclassification rates, and square root mean error).

Given the collinearity that may exist between various functional parameters, we used neural networks (machine learning algorithms) that could dynamically adjust for the relationship between variables, whereas typical regression assumes complete independence or noncollinearity of the inputs. Neural networks can efficiently and flexibly model nonlinear response surfaces. The developed neural networks had the following parameters as inputs: AEX or Sqrt AEX, percent predicted or *z*-scores of FEV_1 and FVC. Output was represented by the functional pattern (based on the classification as normal, obstruction, restriction, or mixed defect). Neural networks were designed with two "hidden" layers, each with three sigmoidal, three linear, and three gaussian distribution nodes, squared penalty method, and up to 50 iteration tours (to avoid overfitting). Internal validation was performed with a random holdback method at a rate of 33%. Statistical significance was set at $P < 0.05$. Analyses were performed using

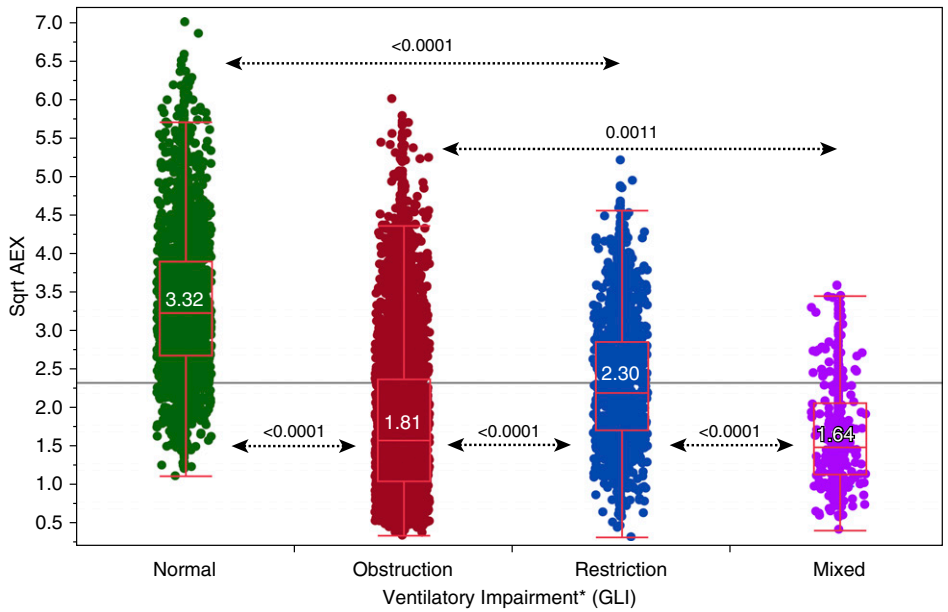

Figure 2. Box-and-whisker plots of the square root of the area under the expiratory flow–volume curve (Sqrt AEX) for Global Lung Initiative (GLI)-defined obstruction, restriction, mixed ventilatory defects, or normal patterns. The numbers associated with the box plots illustrate the mean Sqrt AEX values of each group. Tukey-Kramer and Welch analysis of variance test $P < 0.0001$; in-between group *P* values are shown on the graph. Horizontal gray line: average Sqrt AEX for the entire cohort. *Denotes that small airway disease was not considered as a separate disease category. Color codes: green = normal; red = obstruction; blue = restriction; purple = mixed ventilatory defect (all patterns as determined by GLI predictive equations for spirometry).

JMP Pro14 software (SAS Institute). The study received Institutional Review Board approvals (Cleveland Clinic IRB EX#0504 and EX#19-1129; Emory IRB #00049576/ Atlanta VA R&D Ioachimescu-002).

Results

We analyzed a total of 15,308 consecutive PFTs. Fifty-one percent of the subjects tested were men. Eighty-six percent were (self-identified) white, and 13% were African American. Only 62 subjects self-identified as Hispanic; nevertheless, GLI equations include Hispanic individuals in the same category as white individuals (2). The mean age ± standard deviation of the analyzed subjects was 56 ± 14 years. The helium dilution technique was used to measure lung volumes in 40% of the patients ($n = 8,501$), whereas body plethysmography was used in the remaining 60% ($n = 12,752$).

The main anthropometric and functional parameters of the patients tested are shown in Table 1. By using the manufacturer's proprietary software, the largest acceptable digitally obtained AEX was analyzed (Figure 1).

Using GLI predictive spirometric equations, obstruction was present in 42.6% of the tests. Among those with obstruction, the severity was deemed mild in 7%, moderate in 14%, moderately severe in 14%, severe in 22%, and very severe in 43%. Restriction was confirmed by lung volume testing in 16.5% of the tests, whereas a mixed ventilatory pattern was found in 4.5% of the data set.

The mean Sqrt AEX values were 3.32, 1.81, 2.30, and 1.64 $L \cdot sec^{-0.5}$ in normal, obstruction, restriction, and mixed patterns, respectively; all between-group differences were statistically significant at $P < 0.0011$ levels (Figure 2). The mean Sqrt AEX values were 2.97, 2.30, 1.92, 1.46, and 0.98 $L \cdot sec^{-0.5}$ in mild, moderate, moderately severe, severe, and very severe obstruction, respectively; all between-group differences were significant at $P < 0.0001$.

To assess the ability of AEX to avoid lung volume testing (at least in some cases), we explored the relationship between AEX and IC, IC/TLC, or RV/TLC. As such, in a linear model, the Sqrt AEX was able to predict with good accuracy the IC (Figure 3A). A third-degree polynomial relationship between IC/TLC and Sqrt

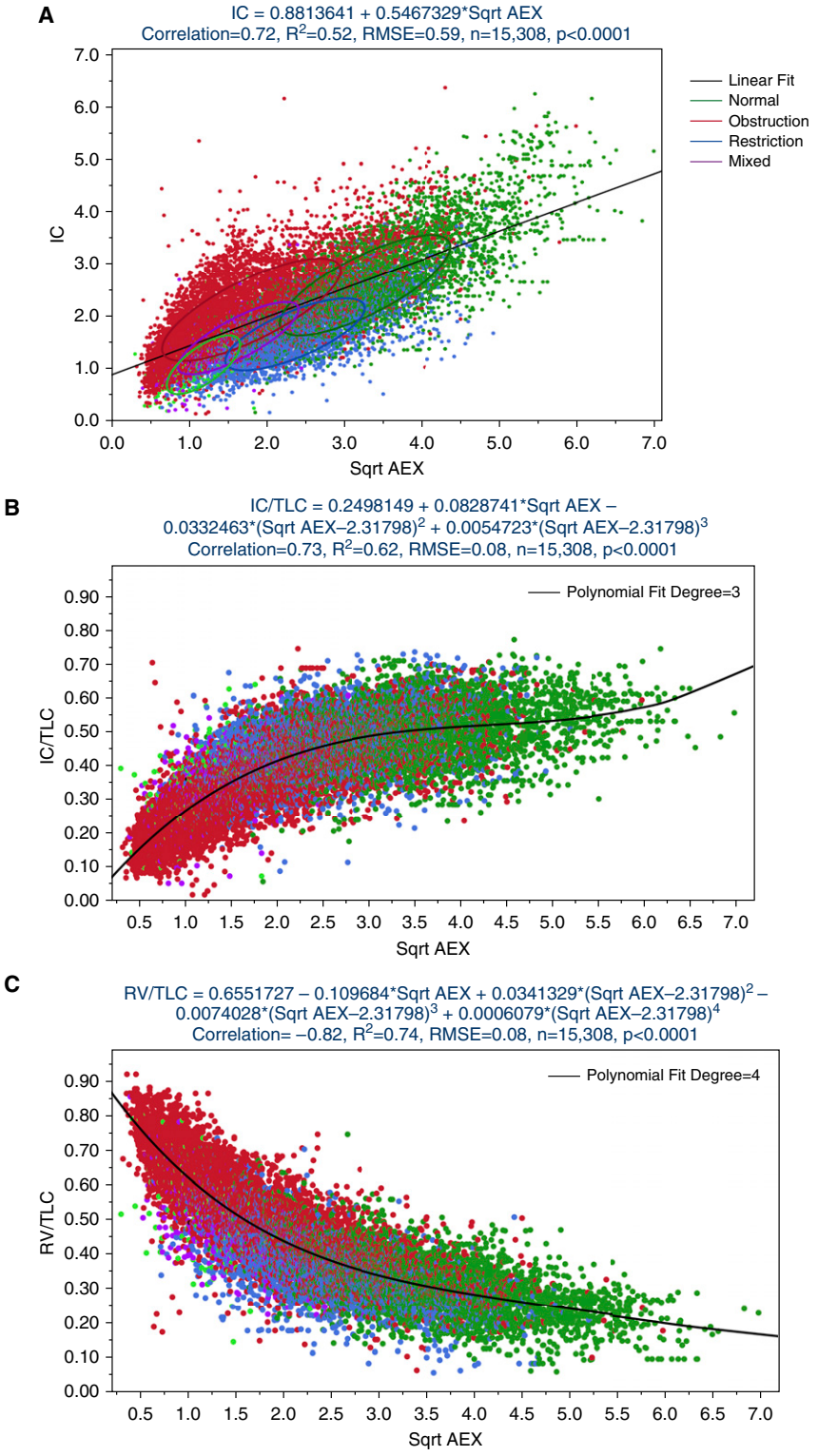

Figure 3. (*A*) Bivariate linear fit of inspiratory capacity (IC) by the square root of the area under the expiratory flow–volume curve (Sqrt AEX). The 50% ellipses are shown for the different Global Lung Initiative (GLI)-defined patterns. (*B*) Bivariate cubic fit of Sqrt AEX by IC/total lung capacity (TLC). (*C*) Bivariate quartic fit of residual volume (RV)/TLC ratio by Sqrt AEX. Color codes: green = normal pattern; red = obstruction; blue = restriction; purple = mixed ventilatory defect; light green = small airway disease (all using GLI reference equations). RMSE = root mean square error.

AEX (Figure 3B) explained approximately two-thirds of the parameter's variance ($R^2 = 0.62$), whereas a quartic fit (fourth-degree polynomial fit) between RV/TLC and Sqrt AEX explained up to three-fourths of the variance ($R^2 = 0.74$) (Figure 3C). As shown in Figures 3A–3C, our cohort included a significant number of patients with very severe obstruction and air trapping, the majority of them being part of a severe emphysema trial.

A simple best-split partition of the diagnostic categories by using FVC and FEV_1 GLI *z*-scores (sex, race, height, and age adjusted) and Sqrt AEX led to a slightly better model performance ($\Delta R^2 = 0.01$–0.02 and lower misclassification rates) than that of the one based on Sqrt AEX plus GLI-based percent predicted FEV_1 and FVC. In Figure 4, we show the expected probabilities of various patterns by using the indicated algorithm in this sample. The model was developed on the basis of 66.6% of the data set ($R^2 = 0.47$) and validated on the basis of 33.3% of the tests ($R^2 = 0.46$). The area under the receiver operating characteristic curve values in both training and validation sets were as follows: 0.98 (in obstruction, restriction, and mixed patterns) and 0.99 (in normal tests).

We also used machine learning (neural network) models to predict the type of GLI-defined ventilatory impairments or patterns (Figure 5). We used as inputs FEV_1, FVC, and FEV_1/FVC ratio *z*-scores (per GLI equations), with or without Sqrt AEX. The model using all four variables showed better performance in differentiating various ventilatory patterns (i.e., lower misclassification rates against standard classifications based on FVC, FEV_1/FVC, and TLC): 8.7% in the training set and 8.4% in the validation set. The lowest concordance rate was for mixed ventilatory defects (48–53%), most of which were misclassified as obstructive patterns. The addition of Sqrt AEX to FEV_1, FVC, and FEV_1/FVC ratio *z*-scores (based on GLI equations) improved overall diagnostic performance by a relatively modest ΔR^2 of 0.01, but, more important, it improved mixed pattern misclassification rates by approximately 20% and 22% in the derivation and validation sets, respectively.

Discussion

The main finding of this study in a large sample of PFTs is that, in combination with traditional spirometric parameters such as FEV_1, FVC, and FEV_1/FVC ratio *z*-scores, AEX performs well in stratifying, both clinically and statistically, the main types and degrees of physiologic derangement, with low overall rates of misclassification (<9%) compared with traditional PFT diagnostic categories.

The appeal of such a parameter is based on the limitations of current interpretive strategies for PFTs. For example, an obstructive ventilatory defect is currently defined by the ATS/ERS Task Force for Standardization of Lung Function Testing (6) as a reduced FEV_1/FVC ratio (i.e., below the fifth percentile of the predicted value). However, it is well known that the earliest changes associated with airflow obstruction in small airways can be seen in the last portion of the flow–volume diagram (with a "concave" or "coved" appearance of the curve), even when the initial portion of FEV_1 is still normal. As another limitation of current interpretive strategies, a restrictive ventilatory defect is defined as having a TLC below the LLN or the fifth percentile of the predicted value, together with a normal FEV_1/FVC ratio. Volumes are typically determined either by gas dilution (e.g., helium method) or by body plethysmography techniques. In practice, spirometry is commonly able to "suggest" restriction, recognizing that a low FVC can reflect either true restriction, airflow obstruction with excessive air trapping and secondary capacity reduction, or early termination of the expiratory effort during the spirometric maneuvers. On this basis, we know that spirometry is generally not able to definitively rule in or rule out restriction, and lung volume determination is generally required (17). Furthermore, a mixed ventilatory defect is characterized by both obstruction and restriction and defined functionally when both FEV_1/FVC and TLC

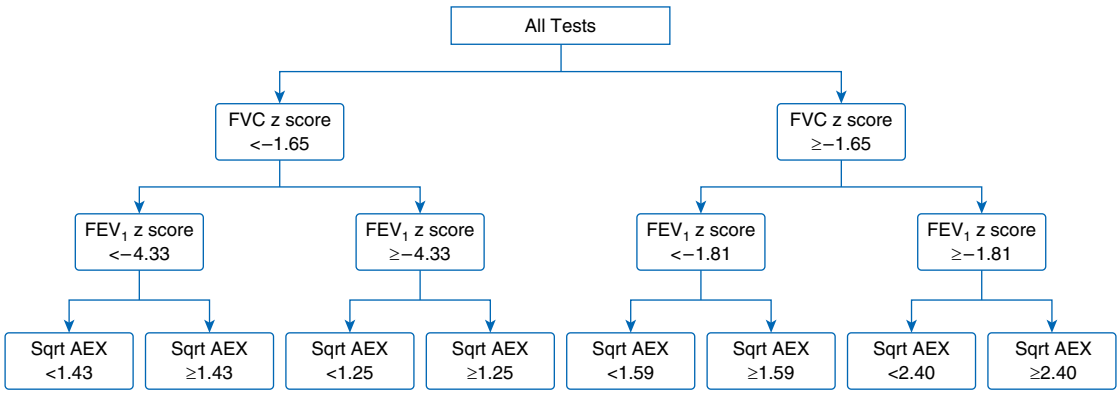

		Sqrt AEX <1.43	Sqrt AEX ≥1.43	Sqrt AEX <1.25	Sqrt AEX ≥1.25	Sqrt AEX <1.59	Sqrt AEX ≥1.59	Sqrt AEX <2.40	Sqrt AEX ≥2.40
Pattern Probability (%)	Normal	0.0	0.0	0.0	0.1	3.2	7.6	75.2	79.3
	Obstruction	84.7	64.0	64.8	38.5	96.8	92.4	24.6	20.7
	Restriction	5.7	21.3	25.2	52.6	0.0	0.0	0.1	0.0
	Mixed	9.6	14.5	10.1	8.9	0.0	0.0	0.0	0.0

Figure 4. Seven-split partition as a proposed pulmonary function test interpretation algorithm based on forced vital capacity (FVC) *z*-score, forced expiratory volume in 1 second (FEV_1) *z*-score, and the square root of the area under the expiratory flow–volume curve (Sqrt AEX). Pattern probability or density refers to the percentage of subjects with the actual spirometric diagnostic categories.

Model Performance (Training Set)

Measures	Value
R^2	0.949
RMSE	0.245
Misclassification Rate	8.7%
AUROC ranges (by patterns)	0.97–0.99
Observations	10,203

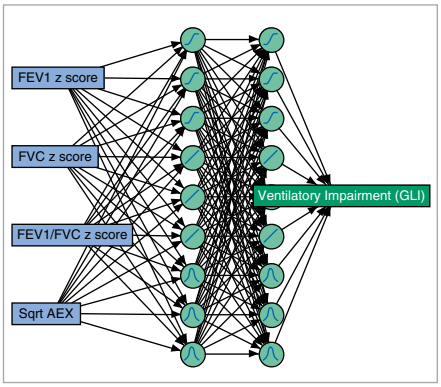

Model Performance (Validation Set)

Measures	Value
R^2	0.949
RMSE	0.244
Misclassification Rate	8.4%
AUROC ranges (by patterns)	0.97–0.99
Observations	5,104

Confusion Matrix (Training Set)

Actual	*Predicted Rate*			
Pattern (GLI)	**Normal**	**Obstruction**	**Restriction**	**Mixed**
Normal	0.997	0.03	0.000	0.000
Obstruction	0.003	0.912	0.068	0.018
Restriction	0.000	0.106	0.893	0.000
Mixed	0.000	0.514	0.005	0.481

Confusion Matrix (Validation Set)

Actual	*Predicted Rate*			
Pattern (GLI)	**Normal**	**Obstruction**	**Restriction**	**Mixed**
Normal	0.995	0.005	0.000	0.000
Obstruction	0.03	0.909	0.070	0.019
Restriction	0.003	0.089	0.907	0.001
Mixed	0.000	0.458	0.013	0.530

Figure 5. Machine learning (neural network) model predicting the type of Global Lung Initiative (GLI)-defined ventilatory impairment (output), using forced expiratory volume in 1 second (FEV_1), forced vital capacity (FVC), and FEV_1/FVC *z*-scores (GLI predicted) and square root transformation of the area under the expiratory flow–volume curve (Sqrt AEX) as inputs. The middle portion of the figure shows the architecture of the neural network, with three inputs, one output, and two layers of intermediary or "hidden" nodes (three linear, three sigmoidal, and three normal distributions). The model showed high performance in differentiating among various ventilatory impairment patterns ($R^2 = 0.949$), with low misclassification rates. The confusion or reclassification matrix summarizes the accuracy and misclassification rates of the model in each actual category. AUROC = area under the receiver operating characteristic curve; RMSE = root mean square error.

are below the fifth percentiles of their predicted values or LLN. As such, because obstructive and restrictive defects can both present with reduced FVC, the presence of a restrictive component in a patient with airflow limitation ("obstructed") cannot always be inferred from the FEV_1 and FEV_1/FVC ratio.

To date, several studies have addressed the possible utility of AEX (8, 11, 18–22). Bunn and colleagues assessed the use of an analog version of AEX and compared it with predicted values based on peak expiratory flow and FVC (8, 18). This was, in fact, almost identical to what we described later as AEX_1 (12). Most studies have addressed pediatric testing (because younger subjects may encounter difficulty comprehending or following instructions), bronchodilator or bronchoconstrictor responses, assessment of "airway patency," or AEX used as a surrogate marker for FEV_1 (also in children) (10, 11, 20–22). Vermaak and colleagues examined the AEX in 60 adult South African subjects without a history of lung disease and derived AEX predictive equations; the study lacked a validation group (19). Four decades later, other authors found that digitally obtained AEX correlated well with hyperinflation in subjects with chronic obstructive pulmonary disease (23), confirming the utility of AEX as a global functional respiratory parameter. Our group is currently in the process of validating predictive equations for AEX, which will allow us in the future to determine age, height, sex, and height-determined AEX *z*-scores, potentially useful in further refinements of diagnostic classifications and severity stratification.

Extending these prior studies that examined AEX in narrow clinical settings or in much smaller populations, in several investigations conducted by our group (9, 12), we have used digital AEX or its approximations as global spirometric measurements of ventilatory impairment in large samples of adults. In these subjects, we validated the existence of obstruction, mixed, or restrictive ventilatory defects by using the gold standard test (i.e., lung volume determination by body plethysmography or by the helium dilution method).

Several limitations of the present study warrant comment. The equations derived (e.g., Figures 3 and 5) are based on a hypothesis-generating set and require validation in an independent, external data set. In addition, the effort to find a better standard for ventilatory impairments such as obstruction, restriction, mixed patterns, or even small airway disease has inherent limitations. For example, the newly proposed measurement may correlate poorly with "imperfect" traditional parameters; it can have significant dependencies (e.g., to FVC) and/or wide coefficients of variation. In this setting, there is still a need to derive and to validate normative data for AEX, a parameter likely influenced by sex, race, height, and possibly even by weight.

The appeal of using neural networks that use spirometric parameters stems from their extraordinary ability in the areas of information processing, their nonlinearity and noise acceptance, and acquisition ("machine learning") and generalization capabilities beyond visible or observable patterns. In contrast to the traditional tools, they offer model-free, adaptive parallel processing and great tolerance for errors, outliers, and data artifacts, which makes them also ideal for normative data derivation in different populations.

Conclusions

The present paper presents the proof of concept and a performance analysis of AEX as an additional instrument derived from spirometry. We found that, in combination with other spirometric measurements, the use of AEX is able to differentiate among traditional diagnostic patterns (normal, obstruction, restriction, or mixed defects). In addition, the AEX could predict with reasonable accuracy IC, IC/TLC, and RV/TLC, potentially obviating the need for more advanced lung function testing such as body plethysmography or gas dilution methods to diagnose hyperinflation, restriction, or mixed defects. Last, using machine learning algorithms with spirometric inputs such as FEV_1, FVC, and FEV_1/FVC ratio *z*-scores in addition to Sqrt AEX significantly improves diagnostic classifications. The low rates of misclassification obtained with this model against traditional functional categories could potentially be employed in epidemiological or population screening studies, in which lung volume determination by body plethysmography or other methods is not practical and spirometry is often the only available testing modality. Further study is needed to validate these findings in larger, independent data sets and to better characterize the relationship between AEX profiles and specific disease endophenotypes. ■

Author disclosures are available with the text of this article at www.atsjournals.org.

Acknowledgment: The authors acknowledge Kevin McCarthy, RCPT, for data extraction.

References

1 American Thoracic Society. Standardization of spirometry: 1994 update. *Am J Respir Crit Care Med* 1995;152:1107–1136.
2 Quanjer PH, Stanojevic S, Cole TJ, Baur X, Hall GL, Culver BH, *et al*.; ERS Global Lung Function Initiative. Multi-ethnic reference values for spirometry for the 3–95-yr age range: the global lung function 2012 equations. *Eur Respir J* 2012;40:1324–1343.
3 Staitieh BS, Ioachimescu OC. Interpretation of pulmonary function tests: beyond the basics. *J Investig Med* 2017;65:301–310.
4 Wanger J, Clausen JL, Coates A, Pedersen OF, Brusasco V, Burgos F, *et al*. Standardisation of the measurement of lung volumes. *Eur Respir J* 2005;26:511–522.
5 American Thoracic Society. Lung function testing: selection of reference values and interpretative strategies. *Am Rev Respir Dis* 1991;144: 1202–1218.
6 Pellegrino R, Viegi G, Brusasco V, Crapo RO, Burgos F, Casaburi R, *et al*. Interpretative strategies for lung function tests. *Eur Respir J* 2005;26: 948–968.
7 Hankinson JL, Odencrantz JR, Fedan KB. Spirometric reference values from a sample of the general U.S. population. *Am J Respir Crit Care Med* 1999;159:179–187.
8 Bunn AE, Vermaak JC, De Kock MA. The area under the maximum expiratory flow–volume curve [abstract]. *Lung* 1978;155:72–73.
9 Ioachimescu OC, McCarthy K, Stoller JK. Alternative measurements to aid interpretation of spirometry: the role of area under the expiratory flow–volume curve (AEX) [abstract]. *Chest* 2006;130:119S.
10 Stein D, Stein K, Ingrisch S. A_{ex} – the area under the expiratory flow-volume loop [in German]. *Pneumologie* 2015;69:199–206.
11 Zapletal A, Chalupová J. Forced expiratory parameters in healthy preschool children (3-6 years of age). *Pediatr Pulmonol* 2003;35: 200–207.
12 Ioachimescu OC, Stoller JK. Area under the expiratory flow-volume curve (AEX): actual versus approximated values. *J Investig Med* 2020; 68:403–411.
13 Coates AL, Peslin R, Rodenstein D, Stocks J. Measurement of lung volumes by plethysmography. *Eur Respir J* 1997;10: 1415–1427.
14 Meneely GR, Kaltreider NL. The volume of the lung determined by helium dilution: description of the method and comparison with other procedures. *J Clin Invest* 1949;28:129–139.
15 Miller MR, Hankinson J, Brusasco V, Burgos F, Casaburi R, Coates A, *et al*.; ATS/ERS Task Force. Standardisation of spirometry. *Eur Respir J* 2005;26:319–338.
16 Crapo RO, Morris AH, Clayton PD, Nixon CR. Lung volumes in healthy nonsmoking adults. *Bull Eur Physiopathol Respir* 1982;18: 419–425.
17 Venkateshiah SB, Ioachimescu OC, McCarthy K, Stoller JK. The utility of spirometry in diagnosing pulmonary restriction. *Lung* 2008;186: 19–25.
18 Bunn AE, De Brandt HM, Vermaak JC. Analogue device for measurement of area under the maximum expiratory flow-volume curve. *Med Biol Eng Comput* 1979;17:695–696.
19 Vermaak JC, Bunn AE, de Kock MA. A new lung function index: the area under the maximum expiratory flow-volume curve. *Respiration* 1979; 37:61–65.
20 Majak P, Cichalewski L, Ożarek-Hanc A, Stelmach W, Jerzyńska J, Stelmach I. Airway response to exercise measured by area under the expiratory flow-volume curve in children with asthma. *Ann Allergy Asthma Immunol* 2013;111:512–515.
21 Zapletal A, Hladíková M, Chalupová J, Svobodová T, Vávrová V. Area under the maximum expiratory flow-volume curve – a sensitive parameter in the evaluation of airway patency. *Respiration* 2008;75: 40–47.
22 Sovijarvi AR. Flow-volume response to inhaled methacholine in asthmatics; comparison of area under the curve (AFV) with conventional parameters. *Eur J Respir Dis Suppl* 1986;143:18–21.
23 Das N, Topalovic M, Aerts JM, Janssens W. Area under the forced expiratory flow-volume loop in spirometry indicates severe hyperinflation in COPD patients. *Int J Chron Obstruct Pulmon Dis* 2019;14:409–418.